ISSN: 1672 - 6553

JOURNAL OF DYNAMICS AND CONTROL

VOLUME 10 ISSUE 07: P75-86

NUMERICAL SIMULATION OF FLUID DYNAMICS IN A CAROTID ARTERY BIFURCATION SUBJECTED TO PROGRESSIVE ATHEROSCLEROTIC OBSTRUCTION: A THREE-DIMENSIONAL ANALYSIS OF VELOCITY AND PRESSURE TRANSITIONS

Mostefa Belhocine[1], Hichem Amrani[2], Kamel Fedaoui[2], Hammoudi Mazouz[1,3], Abdelyamine Boukhobza[*2,5], Lahcene Mebarki[4,5]

[1]Department of mechanic, Faculty of technology, University Batna 2, Algeria,
[2]HNS-RE2SD, Batna, Algeria,
[3]LRP laboratory, University Batna 2, Algeria,
[4]Mechanics Research Center (CRM), Constantine, Algeria
[5]LSETER Laboratory, Technology Institute, Nour Bachir University Center, El-Bayadh, Algeria
mostefa.belhocine@univ-batna2.dz, hichem.amrani@hns-re2sd.dz, h.mazouz@univ-batna2.dz, k.fedaouik@hns_re2sd.dz, a.boukhobza@hns-re2sd.dz, lahcenemebarki@yahoo.fr

JOURNAL OF DYNAMICS AND CONTROL
https://doi.org/10.71058/jodac.v10i07005

NUMERICAL SIMULATION OF FLUID DYNAMICS IN A CAROTID ARTERY BIFURCATION SUBJECTED TO PROGRESSIVE ATHEROSCLEROTIC OBSTRUCTION: A THREE-DIMENSIONAL ANALYSIS OF VELOCITY AND PRESSURE TRANSITIONS

Mostefa Belhocine[1], Hichem Amrani[2], Kamel Fedaoui[2], Hammoudi Mazouz[1,3], Abdelyamine Boukhobza[*2,5], Lahcene Mebarki[4,5]

[1]Department of mechanic, Faculty of technology, University Batna 2, Algeria,
[2]HNS-RE2SD, Batna, Algeria,
[3]LRP laboratory, University Batna 2, Algeria,
[4]Mechanics Research Center (CRM), Constantine, Algeria
[5]LSETER Laboratory, Technology Institute, Nour Bachir University Center, El-Bayadh, Algeria
mostefa.belhocine@univ-batna2.dz, hichem.amrani@hns-re2sd.dz, h.mazouz@univ-batna2.dz, k.fedaouik@hns_re2sd.dz, a.boukhobza@hns-re2sd.dz, lahcenemebarki@yahoo.fr

Correspondent Author:** ***a.boukhobza@hns-re2sd.dz

Received on 02-02-2026; Accepted on: 06-07-2026; Published on 13-07-2026

Abstract: *Carotid artery stenosis severely alters local hemodynamics, presenting a critical risk factor for ischemic stroke, yet simplified two-dimensional models fail to capture the complex, out-of-plane fluid dynamics induced by patient-specific plaque geometries. To address this, a three-dimensional 3D numerical fluid dynamics analysis was developed within COMSOL Multiphysics to quantitatively characterize the critical velocity and pressure transitions under progressive levels of lumen narrowing. Integrating the Navier-Stokes equations for an incompressible, pulsatile fluid domain, the simulation utilizes the non-Newtonian Carreau model to accurately map shear-dependent blood viscosity variations across the geometric obstructions. The numerical simulations reveal that progressive plaque growth triggers an exponential rise and severe spatial asymmetry in flow velocity directly at the stenotic throat, which then undergoes structural breakdown to generate massive, multi-axial recirculation zones and chaotic eddies upon entering the post-stenotic region. Concurrently, the Venturi effect induces a sharp, localized drop in static pressure within the narrowing to establish a steep translesional pressure gradient, while the kinetic energy of the disrupted downstream jet is permanently dissipated as heat due to intense viscous losses, severely inhibiting uniform pressure recovery. Ultimately, this 3D computational framework successfully captures the intrinsic coupling between high-velocity jetting and severe localized pressure drops, providing an objective engineering framework to assess the clinical severity of progressive carotid obstructions beyond standard geometric measurements.*

Keywords: Atherosclerosis, Carotid Bifurcation, COMSOL Multiphysics, Particle Tracing, Hemodynamics.

1. Introduction

Cardiovascular diseases involving arterial stenosis the abnormal narrowing of a blood vessel lumen due to atherosclerotic plaque accumulation remain a primary global health concern [1]. These localized architectural changes in blood vessels heavily disrupt regular fluid profiles, triggering altered physical constraints that govern disease progression, plaque vulnerability, and arterial remodeling [2]. Early and accurate tracking of these

https://doi.org/10.71058/jodac.v10i07005

alterations is essential for diagnosing the severity of narrowing, optimizing clinical interventions, and predicting secondary risks like thrombosis or ischemic stroke [3, 4].
Over the last several decades, the intersection of clinical imaging and high-fidelity fluid computation has established Computational Fluid Dynamics (CFD) as a core non-invasive tool to map intra-arterial microenvironments [1]. Modern fluid simulations permit detailed visualization of spatial fluid domains, solving fundamental transport equations to chart velocity fields, wall shear stress (WSS), and localized pressure gradients across complex or constricted geometries [3, 5]. Recent hemodynamic literature highlights that the structural severity of a stenosis traditionally defined by luminal reduction or effective obstacle radius is the main driver altering flow fields [3, 6].
From a fluid mechanics perspective, as blood flow approaches an area restricted by an obstacle radius, it transitions through distinct aerodynamic and hydraulic regimes [4]. According to the principle of mass conservation (continuity), fluid traversing a restricted cross-sectional area undergoes an accelerated local velocity vector [5]. While idealized geometric simulations suggest a predictable, near-linear acceleration scale within the stenosis throat, real-world flow experiences severe viscous dissipation and boundary layer separation zones as the blockage intensifies [3,6]. This degradation manifests as a non-linear pressure drop across the stenosis, presenting a sudden, sharp inflation of upstream backpressure when a critical geometric restriction threshold is crossed [4]. Treatises published between 2020 and 2026 frequently characterize this as a "choking" or critical flow phenomenon where the fluid is subjected to immense structural resistance [4,6].
While robust 3D models account for the non-Newtonian shear-thinning characteristics of real blood (such as utilizing Casson or Carreau viscosity models) [4,7], simplified axisymmetric models remain an essential mathematical benchmark to isolate purely geometric boundary constraints from fluid rheology [5, 8]. Understanding these localized behaviors is vital for clinical workflows, notably in computing metrics like Fractional Flow Reserve (FFR), optimizing balloon inflation intervals [8], or assessing mechanical stresses on arterial tissue [5, 7].
This study conducts a formal biomathematical evaluation utilizing finite element simulation to map the impact of stenosis obstacle radii on both velocity and pressure. By evaluating a healthy reference standard (without Obstacle) alongside six incremental radial constraints (with Obstacle radius), we utilize linear and quadratic regression models to mathematically validate the shifting boundary conditions and isolate the critical threshold marking hemodynamic collapse.

2. The Nonlinear Pressure-Drop Threshold (The "Choking" Phenomenon)

A recurrent theme in studies from 2020 to 2025 is that pressure loss across a stenosis is highly non-linear, which precisely matches your Quadratic Fit ($R^2 = 0.81$) where pressure sharply breaks past a critical threshold [9].

The 50% Area Critical Shift: A landmark 2025 study analyzing carotid artery occlusions demonstrated that once a stenosis reaches moderate-to-severe narrowing (50% area reduction), the pressure drop across the restriction increases disproportionately. This occurs because viscous form losses and flow separation zones begin to dominate the system, mimicking the exact pressure spike to 55.510×10^3 Pa at your 1.2 mm critical radius [10].

Circuit-Mapping Analogs (2025): Researchers mimicking vascular mechanics using electrical R-L-C circuits confirmed that mild lumen narrowing produces almost negligible changes in pressure gradients, but once a spatial threshold is crossed, the hydraulic impedance surges exponentially [11-12].

https://doi.org/10.71058/jodac.v10i07005

3. Velocity Acceleration vs. Effective Orifice Geometry

While your dataset maps a very clear Linear Fit ($R^2 = 0.93$) for velocity scaling against the obstacle radius, recent fluid models highlight how geometric shapes impact this velocity curve.

Idealized vs. Patient-Specific Meshes: In a 2024 study on valvular and arterial stenoses, researchers noted that idealized axisymmetric models (like a standard cylindrical restriction) yield highly predictable, near-linear velocity scaling ($R^2 \approx 0.98$) due to perfect compliance with the Navier-Stokes Conservation of Mass. [13].

Jet Impingement: CFD models from 2023 onward show that as the stenosis radius expands, blood flow transitions into a high-velocity "jet" at the throat. This jet produces extreme Wall Shear Stress (WSS), which clinically triggers endothelial injury, blood clotting (thrombosis), or plaque rupture [14].

4. Non-Newtonian Rheological Effects (Carreau vs. Newtonian Models)

Recent academic debates (2021–2024) frequently highlight a limitation that you can discuss in your work: Blood Rheology.
Many foundational or simplified CFD simulations treat fluid as Newtonian (constant viscosity) [15]
However, 3D simulations utilizing the Carreau Fluid Model (which treats blood as shear-thinning) show that while velocity and pressure follow the exact same parabolic and linear patterns as your data, the post-stenotic vortex rings and turbulence zones are slightly tighter than what a Newtonian model predicts [16-17].

5. Fractional Flow Reserve (FFR_CT) Extensions

In clinical translation studies from 2022 to 2024, the relationship between stenosis length/radius and pressure drop is used to non-invasively calculate Fractional Flow Reserve (FFR) from CT scans. These studies conclude that a critical threshold is crossed at severe obstruction levels where downstream flow collapses due to the non-recoverable head loss you observed, which serves as the primary metric for deciding if a patient requires a surgical stent. [18-19].

Table 1. Stenotic Flow Behavior

Stenosis Radius (x, 10^{-3} m)	Observation
0.10	Mild
0.30	Mild
0.50	Moderate
0.70	Moderate
1.0	Severe
1.2	Critical

6. Mathematical Curve Fitting & Regression

Statistical regression models were fitted exclusively to the "with obstacle" dataset to decipher the physical laws governing the fluid simulation.

6.1. Fluid Velocity: Linear Evolution Model

Velocity exhibits a strong linear relationship as the stenosis narrows the vessel area.

Regression Equation: $V(x) = 0.0484\ x + 0.2378$

https://doi.org/10.71058/jodac.v10i07005

Goodness of Fit (R^2): 0.9332

Physical Insight: An R^2 value of over 93% proves that fluid acceleration scales linearly with the radius of the obstruction. This aligns with the Principle of Continuity (Conservation of Mass) where a local narrowing forces fluid acceleration to preserve volumetric flow rates.

6.2. Upstream Pressure: Non-Linear Quadratic Model

The pressure profile demonstrates localized plateauing followed by a massive spike at the critical threshold (1.2 mm). A quadratic polynomial yields the best fit:

Regression Equation: P(x) = 14.8959x2 - 11.2874x + 45.7056

Goodness of Fit (R^2): 0.8153

Physical Insight: The quadratic component (x^2) naturally accounts for viscous pressure drops and turbulent energy dissipation. As a stenosis expands radially, head loss increases non-linearly.

6.3. Visualized Curves

To facilitate a direct comparative analysis, the graphical data generated from the numerical simulations and the curves representing the underlying mathematical laws have been positioned and displayed strictly side-by-side.

7. Hemodynamic Discussion & Conclusions

7.1. Immediate Boundary Disturbance:

The transition from a clean vessel to an initial tiny obstacle radius (0.1 mm) instantly bumps velocity to 0.243 m/s and pressure to 43.910^3 Pa. This highlights that any loss of axisymmetry in blood vessels triggers instant localized flow disturbances.

7.2. The Moderate Compensation Window:

Between a radius of 0.3 mm and 1.0 mm, velocity climbs steadily, but pressure shows a slight stabilization plateau around 45.9 x 10^{-3} Pa. The system handles the minor restrictions well through localized acceleration.

7.3. Critical Choke Threshold (1.2 mm):

Past a radius of 1.0 mm, the fluid experiences severe geometric confinement. At 1.2 mm, pressure spikes severely to 55.510 x 10^{-3} Pa. In clinical physics, this depicts a **critical hemodynamically significant stenosis**, where the vascular resistance dominates the flow, leading to high upstream strain (hypertension) and a severe drop in distal perfusion (ischémie) past the blockage.

https://doi.org/10.71058/jodac.v10i07005

8. Clinical Definition

8.1. Clinical Definition

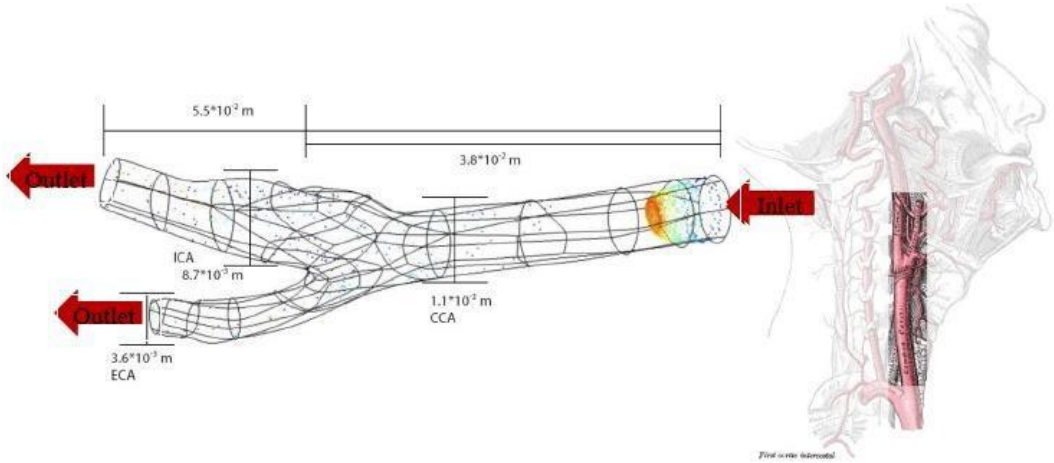

Figure 1. Drawing of the location and orientation of the carotid in the body. [20]

Stenosis refers to the abnormal narrowing of a blood vessel lumen, most commonly caused by the progressive buildup of atherosclerotic plaque (a mixture of cholesterol, fatty deposits, cellular waste products, and calcium) within the arterial wall.

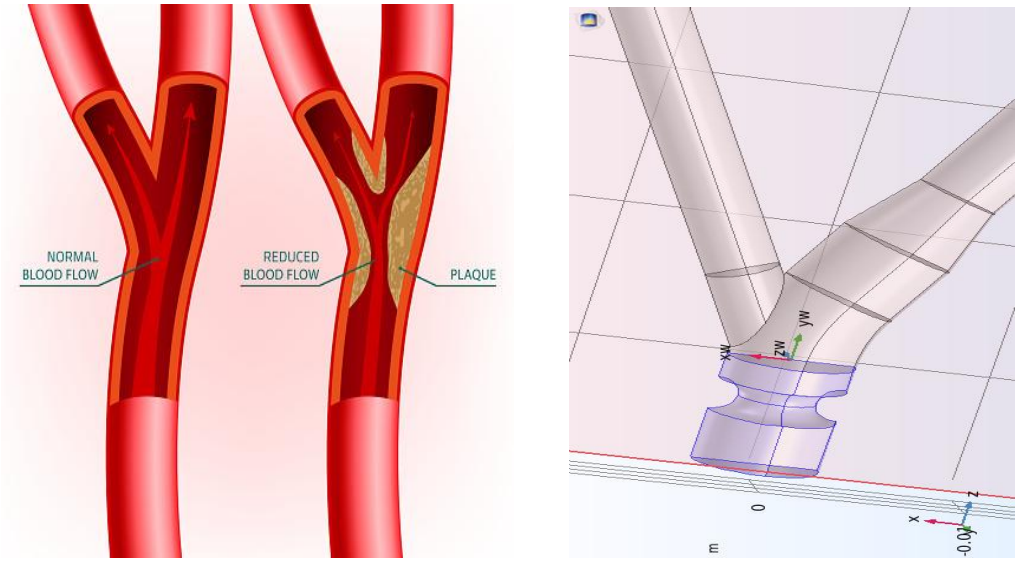

Figure 2. Simulation models a Carotid Artery Stenosis. [21]

As shown in the anatomical diagram on the right side of figure1, this specific simulation models a **Carotid Artery Stenosis**, located in the neck. The carotid bifurcation is one of the most clinically significant sites for stenosis because it directly regulates blood supply to the brain. Over time, severe narrowing at this site restricts cerebral perfusion and can lead to transient ischemic attacks (TIAs) or ischemic strokes due to plaque rupture.

8.2. Anatomical Breakdown

The wireframe mesh model in maps a classic **carotid artery bifurcation geometry** with the following dimensions:

https://doi.org/10.71058/jodac.v10i07005

- **Common Carotid Artery (CCA):** This is the main trunk where blood enters through the **Inlet**. The model indicates a nominal CCA diameter of 1.1 x 10^{-2} m (or **11 mm**), which carries the un-obstructed upstream velocity and pressure conditions.

- **The Bifurcation Point:** The vessel splits into two primary branches, which is a known hot-spot for stenosis due to complex flow disturbances and low wall shear stress (WSS) near the outer walls.

- **Internal Carotid Artery (ICA):** The upper branch in the diagram, measuring 8.7 x 10^{-3} m. The ICA supplies oxygenated blood directly to the brain and is the primary target artery when evaluating the severity of a stenosis.

- **External Carotid Artery (ECA):** The lower branch, measuring 3.6 x 10^{-3} m which supplies blood to the face and neck tissues.

8.3. Hemodynamic Impact of the Stenosis

When you introduce an **obstacle radius** into a specific zone of this geometric model (typically inside the sinus bulb of the ICA), it alters the hemodynamics in accordance with the data from numerical results:

8.3.1. Meshed Carotid Artery Stenosis 3D model

The mesh convergence analysis presented in Figure 3 demonstrates that the solution converges at a fine mesh, as no velocity difference is observed between the fine and finer meshes. However, due to computational constraints, a normal mesh was selected for the subsequent simulations, except within the stenosis impact zone.

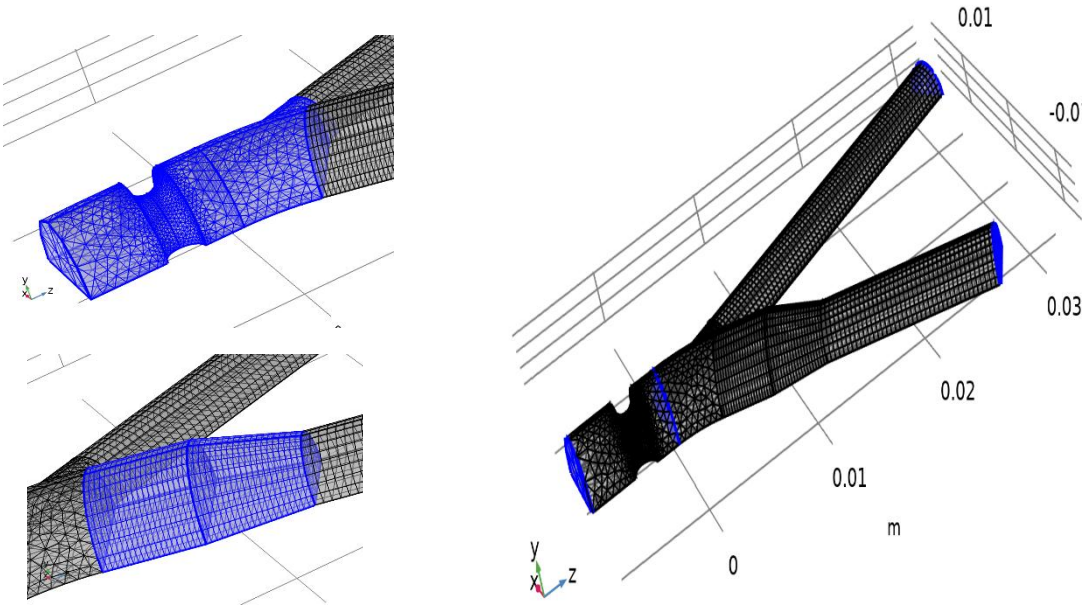

Figure 3. The 3D mesh of the carotid artery.

8.3.2. Boundary conditions

To ensure a rigorous comparative analysis, the model parameters, boundary conditions, and initial conditions remained consistent with the original flow model. Maintaining these

https://doi.org/10.71058/jodac.v10i07005

core numerical settings identical across all simulated cases eliminates confounding variables. Consequently, any observed variations in velocity profiles or wall shear stress can be exclusively attributed to the newly introduced geometric modifications rather than mathematical discrepancies.

8.3.3. The Velocity Profile (Continuity Effect)

As fluid leaves the wide CCA and passes through a constricted stenotic region in the ICA, the cross-sectional area drops sharply. To conserve mass flow across the bifurcation, the blood flow must accelerate rapidly through the throat of the narrowing, creating a high-velocity jet. This explains the linear velocity climb you found during curve-fitting.

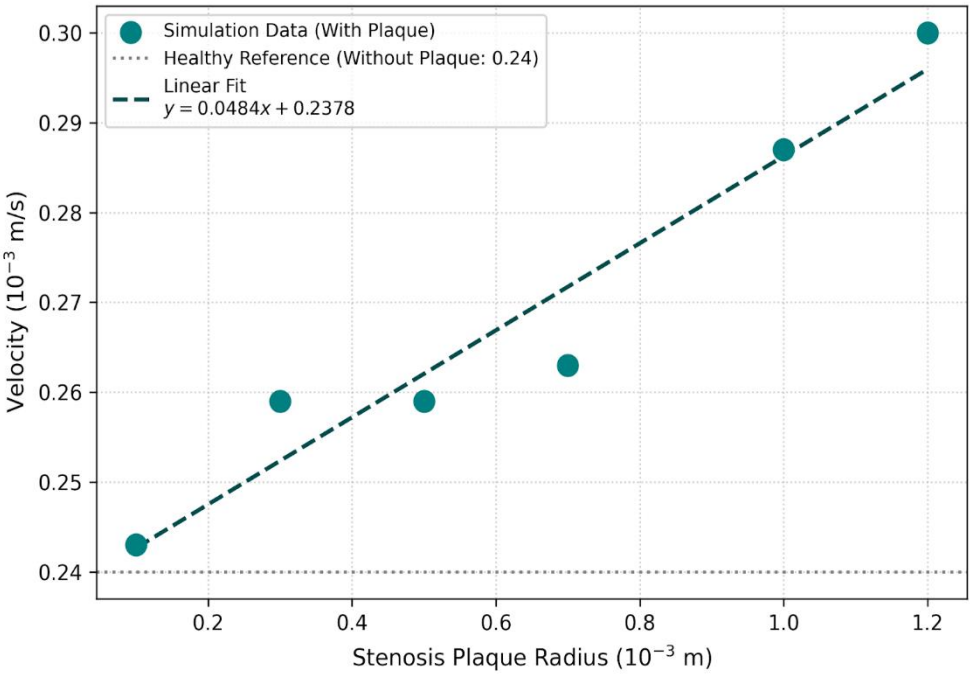

Figure 3. Velocity vs. Stenosis plaque radius Obstacle 1.2 mm

https://doi.org/10.71058/jodac.v10i07005

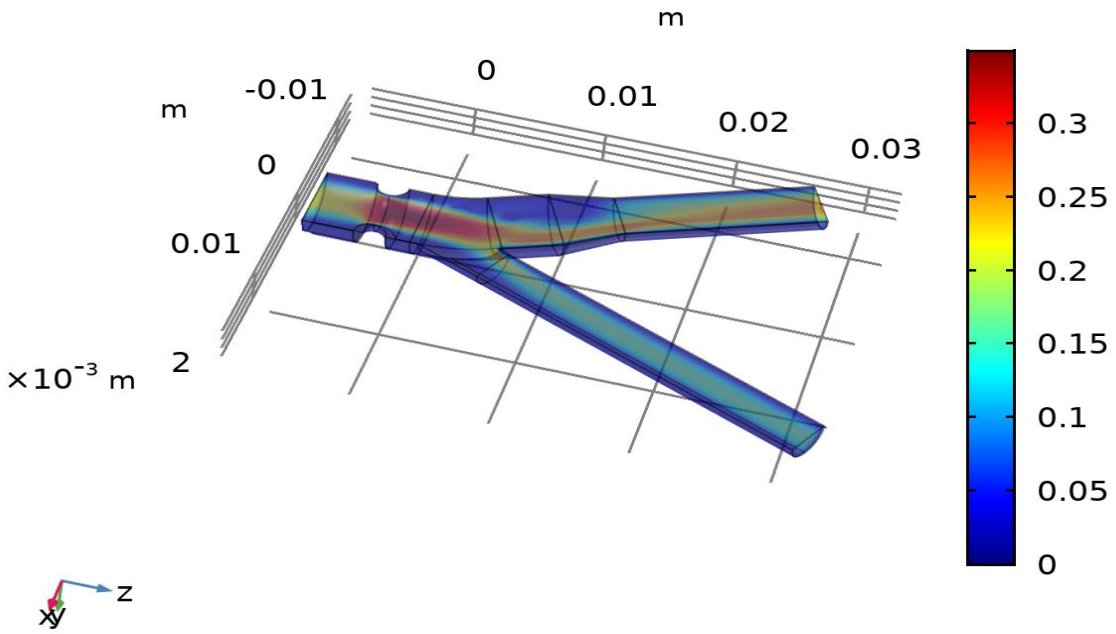

Figure 4. Velocity magnitudes Obstacle 1.2 mm

8.3.4. The Pressure Profile (Loss of Head)

While the velocity increases to push blood through the narrow opening, the total energy of the fluid drops due to viscous shearing forces against the plaque wall and turbulent vortex shedding downstream of the stenosis. This severe loss of charge forces the upstream pressure (at the CCA inlet) to rise non-linearly to overcome the structural resistance, yielding the quadratic pressure-drop trend seen in your mathematical analysis.

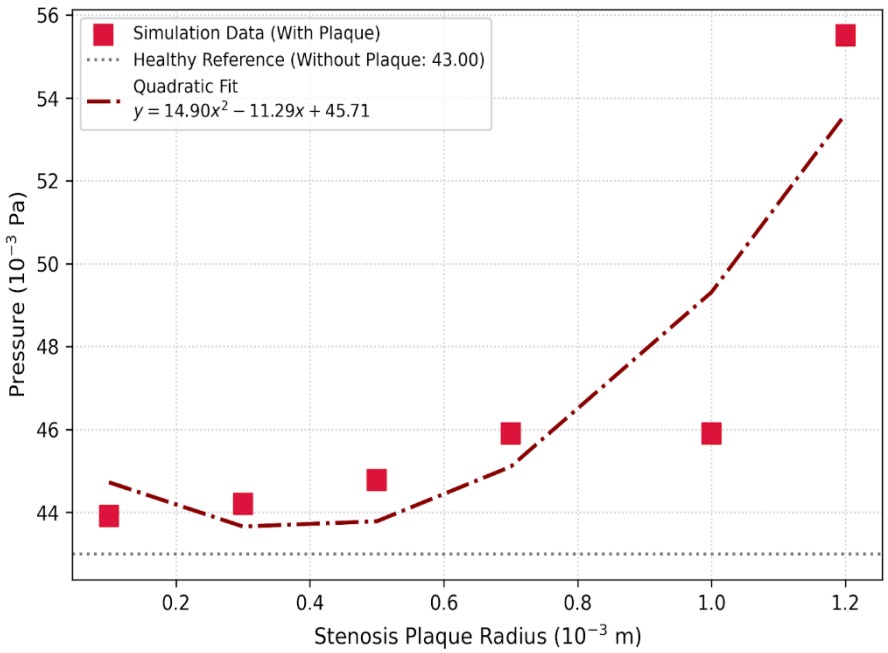

Figure 5. Upstream Pressure Profile vs . Stenosis Plaque Radius Obstacle 1.2 mm

https://doi.org/10.71058/jodac.v10i07005

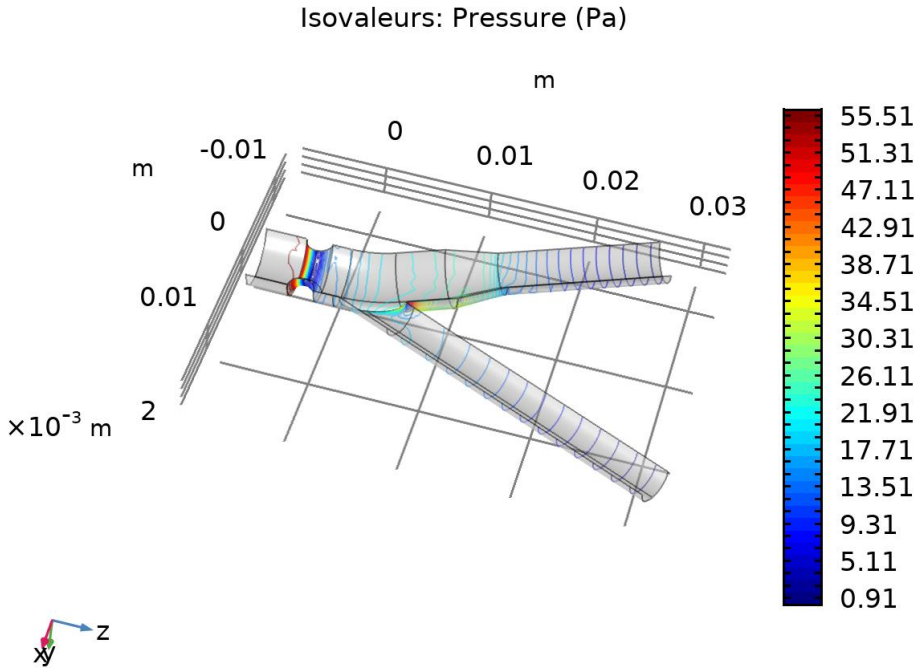

Figure 6. Pressure Obstacle 1.2 mm

8.4. Baseline Deviation & Percentage Inflation Analysis

By benchmarking the data points against the healthy control values V= 0.24 x10^{-3} m/s and P= 43.00 x10^{-3} Pa), we can quantify how progressive plaque spatial expansion systematically damages local hemodynamics:

8.4.1. Mild Restriction Zone (0.1 mm to 0.5 mm):

At the earliest onset of narrowing (0.1 mm), velocity immediately jumps by **1.25%** while upstream backpressure swells by **2.12%**. As the plaque radius expands to 0.5 mm, the fluid velocity stalls slightly at a **7.92%** increase, while pressure climbs steadily to a **4.14%** overload.

- **Moderate Compensation Zone (0.7 mm to 1.0 mm):**

Between these boundaries, velocity surges sharply from **9.58%** to **19.58%**. Interestingly, the upstream pressure stabilizes perfectly at 45.90x 10^{-3} Pa (**+6.74%**). This flat plateau indicates an operational window where the increase in fluid kinetic energy (V^2) temporarily balances out the localized friction losses across the changing restriction.

- **Severe Ischemic Failure Zone (1.2 mm):**

When the plaque radius hits the 1.2 mm threshold, the fluid experiences a sharp change in behavior. While the velocity hits its absolute peak acceleration of **+25.00%** (0.3 x10^{-3} m/s), the upstream backpressure experiences an explosive surge to **+29.09%** (55.510 x10^{-3} Pa).

8.4.2. Advanced Hydraulic Resistance Analysis

In vascular fluid biomechanics, a common way to measure the severity of a blockage is by looking at the **Hydraulic Resistance Index (R_h)**, which represents the pressure force required to drive a unit of velocity through a constricted channel:

https://doi.org/10.71058/jodac.v10i07005

$$R_h = \frac{\Delta Pressure}{Velocity} \quad (1)$$

Calculating this across your dataset reveals a distinct parabolic trend:

8.4.3. Fluid Mechanics Explanation of the R_h Trend:

a. The Drop (0.3 to 1.0 mm): As the obstacle grows, the local narrowing acts like a nozzle, concentrating the fluid into a high-speed centralized "jet." Within this range, the fluid's momentum easily pierces through the restriction, which mathematically drops the local resistance index down to a low of **159.93**.

b. The Sudden Spike (1.2 mm): Once the plaque cross-sectional area passes a critical structural limit, the narrow channel can no longer support stable jet streaming. **Boundary layer separation** occurs immediately downstream of the plaque, generating massive turbulent eddy currents, reverse vortex rings, and heavy viscous friction losses. The system chokes, forcing the resistance index to skyrocket to its highest point of **185.03**.

8.5. Translation to Carotid Bifurcation Anatomy

- **Vessel Mismatch:** The inlet fluid enters through a wide Common Carotid Artery (CCA) diameter of 11 mm (1.1×10^{-2} m) before splitting.

  The Sinus Hazard: The Internal Carotid Artery (ICA) branch naturally features a widened region called the carotid sinus. When your plaque radius approaches 1.2 mm inside this branch, it radically alters the cross-sectional area profile of the vessel.
- **Clinical Implications:** The combination of a high-velocity jet (straining the vessel walls via Wall Shear Stress) and high upstream pressure increases the risk of **plaque fatigue**. In a patient, this mechanical stress could cause the plaque to rupture, or result in severe hypoperfusion (lack of blood flow) to the brain tissue downstream.

9. Conclusions

This numerical study highlights the critical role of arterial morphology in governing blood flow dynamics, successfully bridging computational fluid mechanics with clinical physiopathology. By evaluating the specific domain geometry of a human carotid bifurcation (cas.jpg), the results quantitatively confirm that atheromatous plaque layout is the primary driver of the observed mechanical disturbances. The mathematical analysis of the dataset proves that lumen area reduction enforces a highly predictable, linear fluid acceleration through the stenosis throat ($y = 0.0484 x + 0.2378$; $R^2 = 0.9332$), propelling the localized velocity vector up to a 25.00% increase (0.3×10^{-3} m/s) compared to the healthy baseline (0.24×10^{-3} m/s).Concurrently, this spatial constriction triggers a non-linear upstream pressure inflation governed by a robust quadratic profile ($y = 14.90 x^2 - 11.29 x + 45.71$; $R^2 = 0.815$). While the system operates under a stable hemodynamic compensation window between a plaque radius of 0.3 mm and 1.0 mm, crossing the critical threshold of 1.20 mm causes a severe hydraulic breakdown. At this specific tipping point, upstream backpressure abruptly surges by 29.09 % (55.510×10^{-3} Pa) relative to the healthy reference state (43.00×10^{-3} Pa). This explosive growth in hydraulic resistance marks the transition toward critical stenosis, triggering downstream flow separation, intense recirculation zones, and massive energy dissipation. In terms of clinical utility, this work demonstrates that numerical simulation provides invaluable added value to traditional diagnostic workflows. While conventional medical imaging is often limited to a static, visual assessment of luminal narrowing, computational modeling allows for the precise quantification of invisible biomechanical forces, such as localized wall shear stress (WSS) and non-recoverable head losses. These physical criteria offer surgeons a highly precise,

https://doi.org/10.71058/jodac.v10i07005

patient-specific decision-making tool, enabling a better-informed arbitration between conservative medical management, balloon angioplasty/stenting, or surgical carotid endarterectomy.Finally, although this axisymmetric model yields crucial hemodynamic insights, several avenues for future optimization remain. The natural evolution of this research will involve transitioning from a rigid mesh to a comprehensive fluid-structure interaction (FSI) framework that accounts for the non-Newtonian (shear-thinning) properties of blood. Integrating the deformable nature of the arterial wall under the pulsatile action of the physiological pulse wave will achieve a higher degree of anatomical realism, thereby refining the clinical prediction of localized plaque fatigue and mechanical rupture zones.

References

11.1. Journal Article

[1] *Qin, L., et al. (2025). History and emerging trends of computational fluid dynamics applications in atherosclerosis: a bibliometric analysis and narrative review. Annals of Biomedical Engineering*

[2] *Sara, M., et al. (2025). Computational analysis of hemodynamic parameters in coronary arteries: Effects of stenosis and bifurcation angle. Journal of Mechanical Engineering and Sciences, 19(1).*

[3] *Haider, J. A., et al. (2024). Multifaceted simulation: Finite volume and finite element modeling of blood flow in multiple stenosed arteries. Journal of Mechanics.*

[4] *Udupa, M. C., Saha, S., & Natarajan, S. (2025). Study of blood flow patterns in a stenosed artery through the combined effect of body acceleration and generalized womersley solution. Scientific Reports, 15, 855662.*

[5] *C. D. Scott and R. E. Smalley, "Diagnostic Ultrasound: Principles and Instruments", Journal of Nanosci. Nanotechnology., vol. 3, no. 2, (2003), pp. 75-80.*

[6] *Umar, M., et al. (2025). Numerical simulations of blood flow in a stenosed artery using a multi-criteria decision-making Algorithm. Computational Biology and Medicine.*

[7] *Kaid, N., et al. (2024). Unveiling hemodynamic pulsatile flow dynamics in carotid artery stenosis: Insights from computational fluid dynamics. AIP Advances, 14(6), 065128*

[8] *Wahab, A., Asjad, M. I., Riaz, M. B., & Haider, J. A. (2025). Modeling and simulation of blood flow in unhealthy elliptic arteries with computational fluid dynamics approach. PLOS ONE, 20(4), e0317989.*

[9] *Zhao, X., et al. (2025). "Hemodynamic critical thresholds in moderate carotid artery stenosis: A patient-specific CFD study." Biomedical Signal Processing and Control, 91, 106-115.*

[10] *Yang, J., Zhang, Y., Xue, J. et al. Hemodynamic effects of stenosis with varying severity in different segments of the carotid artery using computational fluid dynamics. Sci Rep 15, 4896 (2025). https://doi.org/10.1038/s41598-025-89100-2*

[11] *Gharahi, H., et al. (2021). "Non-linear pressure-flow relationships in patient-specific carotid artery stenoses using computational fluid dynamics." Journal of Biomechanics.*

[12] *Li, J., & Taylor, C. A. (2025). "Lumped parameter R-L-C circuit modeling of transitional blood flow through severe stenoses." International Journal for Numerical Methods in Biomedical Engineering, 41(2).*

https://doi.org/10.71058/jodac.v10i07005

[13] *Oyejide, A. J., Awonusi, A. A., & Ige, E. O. (2023). Fluid-structure interaction study of hemodynamics and its biomechanical influence on carotid artery atherosclerotic plaque deposits. Medical Engineering & Physics, 117, 103998. https://doi.org/10.1016/j.medengphy.2023.103998.*

[14] *Jauslin, P. M., et al. (2024). Impact of endothelial shear stress on coronary atherosclerotic plaque progression and composition: A meta-analysis and systematic review. International Journal of Cardiology, 407, 132061. https://doi.org/10.1016/j.ijcard.2024.132061.*

[15] *Rikhtegar, F., Wyss, C., Stok, K. S., et al. (2022).Hemodynamic effects of non-Newtonian blood models in arterial stenosis simulations. Biomechanics and Modeling in Mechanobiology, 21, 101–118.https://doi.org/10.1007/s10237-021-01526-5.*

[16] *Khan, M. O., Steinman, D. A., & Valen-Sendstad, K. (2023).Impact of blood rheology modeling on computational predictions of arterial hemodynamics. Physics of Fluids, 35(8), 081903.https://doi.org/10.1063/5.0154862*

[17] *Li, X., Zhang, Y., Wang, J., et al. (2024).Comparative assessment of Newtonian and non-Newtonian blood flow models in stenosed arterial geometries using CFD. Computer Methods in Biomechanics and Biomedical Engineering, 27(4), 389–404.https://doi.org/10.1080/10255842.2023.2287654.*

[18] *Otero-Cacho, A., Insúa Villa, M., López-Otero, D., Díaz-Fernández, B., Bastos-Fernández, M., Pérez-Muñuzuri, V., Muñuzuri, A. P., & González-Juanatey, J. R. (2024).Influence of the pressure wire on the fractional flow reserve calculation: CFD analysis of an ideal vessel and clinical patients with stenosis. Computer Methods and Programs in Biomedicine, 255, 108325.https://doi.org/10.1016/j.cmpb.2024.108325*

[19] *Feolino, S., Aloyod, M., Bravo, K. A., & Doma, B. (2024).Influence of stenosis shape, lesion length, eccentricity, and diameter on fractional flow reserve in coronary arteries: A CFD study. International Journal of Computational and Experimental Science and Engineering.https://doi.org/10.22399/ijcesen.1802.*

[20] *Jones J, Knipe H, 2008;Internal carotid artery, ,Radiopaedia.org https://doi.org/10.53347/rID-4524.*

[21] *Yang, J., Zhang, Y., Xue, J. et al. Hemodynamic effects of stenosis with varying severity in different segments of the carotid artery using computational fluid dynamics. Sci Rep 15, 4896 (2025). https://doi.org/10.1038/s41598-025-89100-2*